Learning to Reconstruct Missing Data from Spatiotemporal Graphs with Sparse Observations

Ivan Marisca[*]
The Swiss AI Lab IDSIA
Università della Svizzera italiana
ivan.marisca@usi.ch

Andrea Cini[*]
The Swiss AI Lab IDSIA
Università della Svizzera italiana
andrea.cini@usi.ch

Cesare Alippi
The Swiss AI Lab IDSIA
Università della Svizzera italiana
Politecnico di Milano
cesare.alippi@usi.ch

Abstract

Modeling multivariate time series as temporal signals over a (possibly dynamic) graph is an effective representational framework that allows for developing models for time series analysis. Spatiotemporal graphs are often highly sparse, with time series characterized by multiple, concurrent, and even long sequences of missing data, e.g., due to the unreliable underlying sensor network. In this context, autoregressive models can be brittle and exhibit unstable learning dynamics. The objective of this paper is to tackle the problem of learning effective models to reconstruct, i.e., *impute*, missing data points by conditioning the reconstruction only on the available observations. In particular, we propose a novel class of attention-based architectures that, given a set of highly sparse discrete observations, learn a representation for points in time and space by exploiting a spatiotemporal propagation architecture aligned with the imputation task. Representations are learned end-to-end to reconstruct observations w.r.t. the corresponding sensor and its neighboring nodes. Compared to the state of the art, our model handles sparse data without propagating prediction errors or requiring a bidirectional model to encode forward and backward time dependencies. Empirical results on representative benchmarks show the effectiveness of the proposed method.

1 Introduction

Exploiting structure – both temporal and spatial – is arguably the key ingredient for the success of modern deep-learning architectures and models. This is the case with spatiotemporal graph neural networks (STGNNs) [1–3], which learn to process multivariate time series while taking into account underlying space and time dependencies by encoding structural spatiotemporal inductive biases in their architectures. However, even when spatiotemporal relationships are present, available data are almost always incomplete and irregularly sampled, both spatially and temporally. This is definitely true for data coming from real sensor networks (SNs), where missing time series observations are usually imputed with simple interpolation strategies before proceeding with the downstream task. More advanced methods deal with missing data by autoregressively replacing missing observations with predicted ones, eventually using bidirectional architectures [4, 5] to exploit both forward and backward temporal dependencies. To account also for spatial dependencies, Cini et al. [6] introduced a method, named GRIN, combining a bidirectional autoregressive architecture with message passing

---

[*]Equal contribution.

neural networks [7–10]. Despite being the state of the art in spatiotemporal imputation, GRIN can suffer from the error propagation typical of autoregressive models [11, 12]. In fact, we argue that the propagation of imputed (biased) values through space and time combined with noisy observations might exacerbate error accumulation in highly sparse data and drive the hidden state of GRIN-like models to drift away.

In this paper, we aim at tackling this problem by designing an architecture based on a novel attention mechanism that takes spatiotemporal sparsity into account while learning representations and imputing missing values. Compared with the alternatives discussed so far, our method exploits a novel spatiotemporal propagation process to learn a predictive representation for each missing observation by relying only on observed values propagated through the spatiotemporal structure. This approach achieves the twofold objective of avoiding propagating biased representation – typical in the autoregressive framework – and reconstructing observations at arbitrary nodes in the sensor network. In summary, our main contributions are:

1. the introduction of a sparse spatiotemporal attention mechanism to learn, from sparse data, representations localized in time and space;

2. the design of a novel STGNN based on the aforementioned spatiotemporal attention mechanism and equipped with inductive biases that make the model tailored for the multivariate time series imputation task;

3. an empirical assessment of the proposed method showing how it overcomes the limits of existing approaches, particularly in settings with highly sparse data.

2 Problem formulation and related works

We denote by $\boldsymbol{X}_t \in \mathbb{R}^{N \times d}$ the matrix collecting the d-dimensional measurements of N sensors (or measurement stations) in a SN at time step t, with $\boldsymbol{X}_{t:t+T}$ being the sequence of T measurements collected in the time interval $[t, t + T)$. We model functional relationships among the sensors as graph edges, represented by the weighted adjacency matrix $\boldsymbol{A} \in \mathbb{R}^{N \times N}$, in which each nonzero entry $a^{i,j}$ indicates the weight of the edge going from the i-th node to the j-th. We assume to have available sensor-level covariates $\boldsymbol{Q}_t \in \mathbb{R}^{N \times d_q}$ that act as spatiotemporal coordinates to localize a point in time and space (e.g., date/time features and geographic location). To account for data availability, we use a binary mask $\boldsymbol{m}_t \in \{0,1\}^N$ whose i-th element m_t^i is 1 if the measurements associated with the i-th sensor are valid at time step t. Conversely, if $m_t^i = 0$, we consider the measurements $\boldsymbol{x}_t^i$ to be completely missing, with the exogenous variables $\boldsymbol{q}_t^i$ being instead available. Finally, we model the multivariate, structured time series as a discrete sequence of graphs, where each graph is a tuple $\mathcal{G}_t = \langle \boldsymbol{X}_t, \boldsymbol{Q}_t, \boldsymbol{m}_t, \boldsymbol{A} \rangle$. Denoting by $\widetilde{\boldsymbol{X}}_{t:t+T}$ the unknown corresponding complete sequence, the goal of multivariate time series imputation (MTSI) is to find an estimate $\widehat{\boldsymbol{X}}_{t:t+T}$ minimizing the reconstruction error over the missing data points. Notice that, since $\widetilde{\boldsymbol{X}}_{t:t+T}$ is not available, one should find a surrogate objective or simulate the presence of missing data, for which the reconstruction error can be computed.

Related works. Multivariate time series imputation is a core task in time series analysis and deep learning methods are commonly used in this regard. In particular, deep autoregressive models based on recurrent neural networkss (RNNs) are currently among the most widely adopted methods [4, 5, 13, 14]. Several approaches in the literature, then, rely on generative adversarial neural networks [15] to generate imputed subsequences by matching the underlying data distribution [14, 16, 17]. Recently, several attention-based imputation techniques have also been proposed [18–20]. More related to our work, GRIN [6] uses a bidirectional graph RNN with a message passing spatial decoder, to impute time series based on spatiotemporal dependencies. The attention mechanism [21, 22] has been exploited in several contexts within the graph deep learning literature [23–26]. In particular, TraverseNet [27] is specially related to our work, since it relies on spatiotemporal autoregressive attention to compute messages exchanged between nodes.
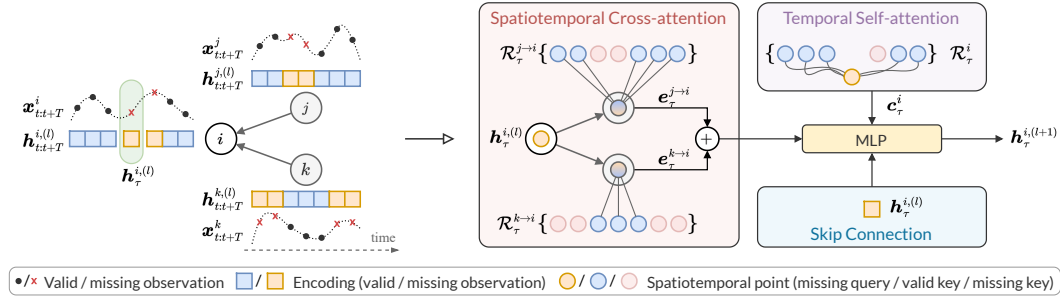
3 Methodology

The autoregressive approach to reconstruction consists in directly modeling distributions $p\left(\boldsymbol{x}_t^i \mid \boldsymbol{X}_{<t}\right)$, with $\boldsymbol{X}_{<t}$ being the sequence of observations prior to time step t, and using one-step-ahead forecasting

as a surrogate objective to learn how to recover missing observations. To also consider $\boldsymbol{X}_{>t}$, i.e., data subsequent to the target time step, it is common to use a bidirectional architecture which models also $p\big(\boldsymbol{x}_t^i \,|\, \boldsymbol{X}_{>t}\big)$ [5, 28]. Moreover, a third component $p\big(\boldsymbol{x}_t^i \,|\, \{\boldsymbol{x}_t^{j\neq i}\}\big)$ must be introduced to account for spatial information at each step. Architectures like GRIN, follow exactly this scheme with different components dedicated to model each of these three aspects. While being effective in practice, these approaches can have multiple drawbacks. Besides the computational overhead of having three separate components and the compounding error in the autoregressive models [11, 12], they can fall short in capturing global context, as the processing of the structural information is decomposed. Furthermore, merging the information coming from the different modules is also problematic, yielding to further compounding of errors. Finally, in the case of highly sparse observations, the spatial processing should be dealt with special care as propagating information through partially observed spatiotemporal graphs adds another layer of complexity.

Our approach, named *Spatiotemporal Point Inference Network* (SPIN), is a graph attention network for MTSI, designed to learn representations of discrete points associated with nodes of a sequence of spatiotemporal graphs. We denote as *observed set* $\mathcal{X}_{t:t+T} = \big\{ \langle \boldsymbol{x}_\tau^i, \boldsymbol{q}_\tau^i \rangle \,|\, m_\tau^i = 1 \wedge \tau \in [t, t+T) \big\}$ the set of all observations, paired with their spatiotempotal coordinates. Conversely, we name *target set* $\mathcal{Y}_{t:t+T} = \big\{ \boldsymbol{q}_\tau^i \,|\, m_\tau^i = 0 \wedge \tau \in [t, t+T) \big\}$ the complement set collecting the coordinates of the discrete spatiotemporal points for which we want to reconstruct an observation. Then, for all discrete points $\boldsymbol{q}_\tau^i \in \mathcal{Y}_{t:t+T}$, SPIN is trained to learn a model

$$f_\theta(\boldsymbol{q}_\tau^i \,|\, \mathcal{X}_{t:t+T}, \boldsymbol{A}) \approx \mathbb{E}\left[p\big(\boldsymbol{x}_\tau^i \,|\, \boldsymbol{q}_\tau^i, \mathcal{X}_{t:t+T}, \boldsymbol{A}\big) \right]. \tag{1}$$

To this end, SPIN learns a parameterized propagation process where each representation, corresponding to a node and time step, is updated by aggregating information from all the available observations acquired at neighboring nodes, weighted by input-dependent attention scores. The core component of SPIN is a novel *sparse spatiotemporal attention* layer (Figure 1) used to propagate information at the level of single observations. Indeed, leveraging on the attention mechanism, we learn representations for each i-th node at each τ-th time step by simultaneously aggregating information from (1) the observed set of i-th node $\mathcal{X}_{t:t+T}^i$; (2) the observed set $\mathcal{X}_{t:t+T}^j$ of each $j \in \mathcal{N}(i)$, i.e., the set of neighbors of the i-th node.

Figure 1: Example of the sparse spatiotemporal attention layer acting for updating $\boldsymbol{h}_\tau^{i,(l)}$, by simultaneously performing inter-node spatiotemporal cross-attention and intra-node temporal self-attention.

Let $\boldsymbol{h}_\tau^{i,(l)} \in \mathbb{R}^{d_h}$ be the learned representation for the i-th node and time step τ at the l-th layer. The encoding is initialized as $\mathrm{MLP}\big(\boldsymbol{x}_\tau^i, \boldsymbol{q}_\tau^i\big)$ if observation $\boldsymbol{x}_\tau^i$ is valid, or $\mathrm{MLP}\big(\boldsymbol{q}_\tau^i\big)$ otherwise, where MLP is a multi-layer perceptron. The next steps involve computations of spatiotemporal messages, i.e., representations computed to propagate information from one discrete space-time point to another. We indicate the propagation along the temporal dimension from time step s to time step τ as subscripts $s \to \tau$. Similarly, superscripts $j \to i$ indicate messages sent from the j-th node to the i-th. To avoid overloading the notation, we omit the layer superscript in the following. The message $\boldsymbol{r}_{s\to\tau}^{j\to i} \in \mathbb{R}^{d_h}$ from the j-th node at time step s to the i-th node at time step τ is computed with an MLP taking as input both source and target representations (Eq. 2). To account for spatial information, this mechanism is used to perform an *inter-node* temporal cross-attention, computing a message to $\boldsymbol{h}_\tau^i$ using encodings in $\boldsymbol{h}_{t:t+T}^j$ associated with a valid observation for every neighbor $j \in \mathcal{N}(i)$ (Eq. 3).

$$\boldsymbol{r}_{s\to\tau}^{j\to i} = \mathrm{MLP}\big(\boldsymbol{h}_s^j, \boldsymbol{h}_\tau^i\big) \qquad (2) \qquad \mathcal{R}_\tau^{j\to i} = \{\boldsymbol{r}_{s\to\tau}^{j\to i} \,|\, \langle \boldsymbol{x}_s^j, \boldsymbol{q}_s^j \rangle \in \mathcal{X}_{t:t+T}\} \qquad (3)$$

Messages in $\mathcal{R}_\tau^{j\to i}$ are then weighted by *message scores* $\alpha_{s\to\tau}^{j\to i}$, computed by a linear projection of

Table 1: Performance (MAE) with increasing data sparsity (average over 5 evaluation masks).

	METR-LA			PEMS-BAY			AQI		
	5 %	10 %	15 %	5 %	10 %	15 %	5 %	10 %	15 %
BRITS	5.87 ± 0.03	7.26 ± 0.06	8.29 ± 0.07	4.14 ± 0.05	5.41 ± 0.08	5.84 ± 0.04	24.09 ± 0.30	31.90 ± 0.26	37.62 ± 0.42
SAITS	4.73 ± 0.07	6.66 ± 0.05	7.27 ± 0.03	3.88 ± 0.09	7.62 ± 0.21	8.01 ± 0.11	20.78 ± 0.30	30.16 ± 0.39	36.34 ± 0.33
Transformer	6.03 ± 0.04	7.19 ± 0.05	8.06 ± 0.05	3.69 ± 0.06	5.09 ± 0.05	6.02 ± 0.04	29.21 ± 0.33	33.62 ± 0.16	37.31 ± 0.14
GRIN	3.05 ± 0.02	4.52 ± 0.05	5.82 ± 0.06	2.26 ± 0.03	3.45 ± 0.06	4.35 ± 0.04	15.62 ± 0.24	22.08 ± 0.39	29.03 ± 0.42
SPIN	2.71 ± 0.02	3.32 ± 0.02	3.87 ± 0.05	$\mathbf{1.78 \pm 0.03}$	$\mathbf{2.15 \pm 0.03}$	$\mathbf{2.41 \pm 0.02}$	$\mathbf{14.29 \pm 0.24}$	$\mathbf{18.71 \pm 0.34}$	$\mathbf{24.34 \pm 0.46}$
SPIN-H	$\mathbf{2.64 \pm 0.02}$	$\mathbf{3.17 \pm 0.02}$	$\mathbf{3.61 \pm 0.04}$	$\mathbf{1.75 \pm 0.04}$	2.16 ± 0.03	2.48 ± 0.02	14.55 ± 0.26	19.37 ± 0.36	25.38 ± 0.37

the messages in $\mathcal{R}_\tau^{j \to i}$ followed by a softmax layer, and aggregated to obtain an edge-level context vector $\boldsymbol{e}_\tau^{j \to i}$, encoding the observed sequence at each j-th node w.r.t. the i-th node and time step τ. Analogously, to account for the observed sequence of the i-th node itself, we exploit an *intra-node* temporal self-attention mechanism to compute messages from the encodings $\boldsymbol{h}_{t:t+T}^i$ corresponding to valid observations, aggregated (weighted by message scores) to obtain a temporal context vector $\boldsymbol{c}_\tau^i$. Then, target representation $\boldsymbol{h}_\tau^{i,(l)}$ is updated with a final aggregation step (Eq. 4), and imputations for all spatiotemporal points in $\mathcal{Y}_{t:t+T}$ are obtained – after L layers – with a nonlinear readout (Eq. 5).

$$\boldsymbol{h}_\tau^{i,(l+1)} = \mathrm{MLP}\Big(\boldsymbol{h}_\tau^{i,(l)},\ \boldsymbol{c}_\tau^{i,(l)},\ \sum\nolimits_{j \in \mathcal{N}(i)} \boldsymbol{e}_\tau^{j \to i,(l)}\Big) \tag{4}$$

$$\widehat{\mathcal{Y}}_{t:t+T} = \{\hat{\boldsymbol{x}}_\tau^i = \mathrm{MLP}\big(\boldsymbol{h}_\tau^{i,(L)}\big) \,|\, \boldsymbol{q}_\tau^i \in \mathcal{Y}_{t:t+T}\} \tag{5}$$

Hierarchical attention. Roughly speaking, the proposed spatiotemporal attention mechanism can be viewed as performing attention over the spatiotemporal graph $\mathcal{S}$, obtained by considering the product graph between space and time dimensions. Performing graph attention on the surrogate graph $\mathcal{S}$ has time and memory complexities that scale with $O((N + E)T^2)$, with N, E being the largest number of nodes and edges, respectively, among graphs in $\mathcal{G}_{t:t+T}$. To reduce this computational burden – which undermines the application of the proposed method to large graphs and long time horizons – we propose to rewire the attention mechanism to be hierarchical [29]. We do this by adding K dummy nodes that act as hubs for propagating information. In this way, we can reduce the spatiotemporal attention complexity to $O((N + E)KT)$, with $K \ll T$, at the cost of introducing an information bottleneck. We refer to Appendix B for a detailed explanation of this mechanism.

4 Empirical evaluation

In this section, we evaluate our method on three real-world datasets and compare the performance against state-of-the-art methods and standard approaches for MTSI. In following experiment, we consider both **SPIN** and the hierarchical version **SPIN-H**. The figure of merit used is the *mean absolute error* (MAE), averaged across imputation windows. We consider only the *out-of-sample* scenario similarly to previous works [6], in which every parametric model is trained and tested on disjoint sets. We consider three openly available datasets coming from real-world SNs. The first two, namely **PEMS-BAY** and **METR-LA** [2], record traffic measurements and are both widely used benchmarks in spatiotemporal forecasting literature. We use the same setup of [6] to inject missing data with *Point missing* policy, in which we randomly drop 25% of the available data. As a third dataset, we consider **AQI** [30, 31], which collects hourly measurements of air pollutants from 437 air quality monitoring stations in China. We consider also a smaller version of this dataset (**AQI-36**) with only the 36 sensors in the city of Beijing. We use the same missing data distribution used in [6, 31]. In all settings, all the valid observations masked out are used as targets for evaluation. We obtain an adjacency matrix from the pairwise distance of sensors following previous works [2, 3, 6]. We compare our methods against (1) GRIN [6], a graph-based bidirectional RNN for MTSI with state-of-the-art performance; (2) a spatiotemporal Transformer, where we alternate temporal and spatial Transformer encoder layers from [21] and replace missing values with a [MASK] token (as in [32]); (3) SAITS [18], a recent attention-based architecture; (4) BRITS [5], which leverages on a bidirectional RNN. We assess how performance changes as the percentage of missing values increases. In practice, we change the missing data distribution at test time, simulating the case in which, at each time step, every sensor has a constant probability $\bar{p}$ of going offline for a random number $S \sim \mathcal{U}(12, 36)$ of future (consecutive) time steps. Table 1 shows results for all datasets with $\bar{p} = 5\%$, $\bar{p} = 10\%$, and

$\bar{p} = 15\%$. Note that, depending on the dataset, the portion of valid observations in each of these cases amounts to $\approx$ 25-30%, $\approx$ 8-10%, and $\approx$ 3-4%, respectively. SPIN models, differently from the baselines, can handle all the considered scenarios. In particular, improvements in performance w.r.t. the best performing baseline (GRIN) are more evident as the number of available observations decreases. Indeed, the sparse spatiotemporal attention mechanism of SPIN is not autoregressive and allows an unbounded memory capacity. Note also that SPIN-H performs on par (and in some cases better) with SPIN, making it a valid lightweight alternative to SPIN. In Appendix A, we show that SPIN-based models perform on par or better than state-of-the-art methods on standard benchmarks. The code to reproduce the experiments of the paper is available online[2].

5   Conclusions

We introduced a graph-based attention network, named SPIN, to reconstruct missing observations in sparse spatiotemporal time series. We showed how the time and space complexities of the approach can be drastically reduced by considering a novel hierarchical attention mechanism. Empirical analysis shows that the proposed method widely outperforms state-of-the-art methods for imputation in highly sparse settings. Future works could investigate the application of SPIN in other time series analysis tasks (e.g., forecasting), as well as in settings with an underlying dynamic graph topology.

Author Contributions

The authors' contributions to this work are specified as follows, adopting the Contributor Roles Taxonomy (CRediT):

- Ivan Marisca: Conceptualization, Data curation, Formal Analysis, Investigation, Methodology, Software, Validation, Visualization, Writing – original draft, Writing – review & editing.
- Andrea Cini: Conceptualization, Data curation, Formal Analysis, Investigation, Methodology, Software, Validation, Visualization, Writing – original draft, Writing – review & editing.
- Cesare Alippi: Conceptualization, Formal Analysis, Funding acquisition, Methodology, Project administration, Resources, Supervision, Writing – original draft, Writing – review & editing.

Acknowledgements

References

[1] Youngjoo Seo, Michaël Defferrard, Pierre Vandergheynst, and Xavier Bresson. Structured sequence modeling with graph convolutional recurrent networks. In *International Conference on Neural Information Processing*, pages 362–373. Springer, 2018. 1

[2] Yaguang Li, Rose Yu, Cyrus Shahabi, and Yan Liu. Diffusion convolutional recurrent neural network: Data-driven traffic forecasting. In *International Conference on Learning Representations*, 2018. 4

[3] Zonghan Wu, Shirui Pan, Guodong Long, Jing Jiang, and Chengqi Zhang. Graph wavenet for deep spatial-temporal graph modeling. *arXiv preprint arXiv:1906.00121*, 2019. 1, 4, 10

[4] Jinsung Yoon, William R Zame, and Mihaela van der Schaar. Multi-directional recurrent neural networks: A novel method for estimating missing data. In *Time Series Workshop at the 34th International Conference on Machine*, pages 1–5, 2017. 1, 2

[5] Wei Cao, Dong Wang, Jian Li, Hao Zhou, Yitan Li, and Lei Li. Brits: bidirectional recurrent imputation for time series. In *Proceedings of the 32nd International Conference on Neural Information Processing Systems*, pages 6776–6786, 2018. 1, 2, 3, 4

---

[2]https://github.com/Graph-Machine-Learning-Group/spin

[6] Andrea Cini, Ivan Marisca, and Cesare Alippi. Filling the g_ap_s: Multivariate time series imputation by graph neural networks. In *International Conference on Learning Representations*, 2022. URL https://openreview.net/forum?id=kOu3-S3wJ7. 1, 2, 4, 8, 9, 10

[7] Franco Scarselli, Marco Gori, Ah Chung Tsoi, Markus Hagenbuchner, and Gabriele Monfardini. The graph neural network model. *IEEE transactions on neural networks*, 20(1):61–80, 2008. 2

[8] Michael M Bronstein, Joan Bruna, Yann LeCun, Arthur Szlam, and Pierre Vandergheynst. Geometric deep learning: going beyond euclidean data. *IEEE Signal Processing Magazine*, 34 (4):18–42, 2017.

[9] Justin Gilmer, Samuel S Schoenholz, Patrick F Riley, Oriol Vinyals, and George E Dahl. Neural message passing for quantum chemistry. In *International conference on machine learning*, pages 1263–1272. PMLR, 2017.

[10] Peter W Battaglia, Jessica B Hamrick, Victor Bapst, Alvaro Sanchez-Gonzalez, Vinicius Zambaldi, Mateusz Malinowski, Andrea Tacchetti, David Raposo, Adam Santoro, Ryan Faulkner, et al. Relational inductive biases, deep learning, and graph networks. *arXiv preprint arXiv:1806.01261*, 2018. 2

[11] Samy Bengio, Oriol Vinyals, Navdeep Jaitly, and Noam Shazeer. Scheduled sampling for sequence prediction with recurrent neural networks. *Advances in neural information processing systems*, 28, 2015. 2, 3

[12] Yukai Liu, Rose Yu, Stephan Zheng, Eric Zhan, and Yisong Yue. Naomi: Non-autoregressive multiresolution sequence imputation. *Advances in Neural Information Processing Systems*, 32: 11238–11248, 2019. 2, 3

[13] Zhengping Che, Sanjay Purushotham, Kyunghyun Cho, David Sontag, and Yan Liu. Recurrent neural networks for multivariate time series with missing values. *Scientific reports*, 8(1):1–12, 2018. 2

[14] Xiaoye Miao, Yangyang Wu, Jun Wang, Yunjun Gao, Xudong Mao, and Jianwei Yin. Generative semi-supervised learning for multivariate time series imputation. In *Proceedings of the AAAI Conference on Artificial Intelligence*, volume 35, pages 8983–8991, 2021. 2, 8

[15] Ian Goodfellow, Jean Pouget-Abadie, Mehdi Mirza, Bing Xu, David Warde-Farley, Sherjil Ozair, Aaron Courville, and Yoshua Bengio. Generative adversarial nets. *Advances in neural information processing systems*, 27, 2014. 2

[16] Jinsung Yoon, James Jordon, and Mihaela Schaar. Gain: Missing data imputation using generative adversarial nets. In *International Conference on Machine Learning*, pages 5689–5698. PMLR, 2018. 2, 8

[17] Yonghong Luo, Ying Zhang, Xiangrui Cai, and Xiaojie Yuan. E²gan: End-to-end generative adversarial network for multivariate time series imputation. In *Proceedings of the Twenty-Eighth International Joint Conference on Artificial Intelligence, IJCAI-19*, pages 3094–3100. International Joint Conferences on Artificial Intelligence Organization, 7 2019. 2

[18] Wenjie Du, David Côté, and Yan Liu. Saits: Self-attention-based imputation for time series. *arXiv preprint arXiv:2202.08516*, 2022. 2, 4

[19] Yusuke Tashiro, Jiaming Song, Yang Song, and Stefano Ermon. Csdi: Conditional score-based diffusion models for probabilistic time series imputation. *Advances in Neural Information Processing Systems*, 34, 2021.

[20] Satya Narayan Shukla and Benjamin Marlin. Multi-time attention networks for irregularly sampled time series. In *International Conference on Learning Representations*, 2020. 2

[21] Ashish Vaswani, Noam Shazeer, Niki Parmar, Jakob Uszkoreit, Llion Jones, Aidan N Gomez, Łukasz Kaiser, and Illia Polosukhin. Attention is all you need. In *Advances in neural information processing systems*, pages 5998–6008, 2017. 2, 4

[22] Dzmitry Bahdanau, Kyunghyun Cho, and Yoshua Bengio. Neural machine translation by jointly learning to align and translate. *arXiv preprint arXiv:1409.0473*, 2014. 2

[23] Kiran K Thekumparampil, Chong Wang, Sewoong Oh, and Li-Jia Li. Attention-based graph neural network for semi-supervised learning. *arXiv preprint arXiv:1803.03735*, 2018. 2

[24] Petar Veličković, Guillem Cucurull, Arantxa Casanova, Adriana Romero, Pietro Liò, and Yoshua Bengio. Graph attention networks. In *International Conference on Learning Representations*, 2018.

[25] Jiani Zhang, Xingjian Shi, Junyuan Xie, Hao Ma, Irwin King, and Dit Yan Yeung. Gaan: Gated attention networks for learning on large and spatiotemporal graphs. In *34th Conference on Uncertainty in Artificial Intelligence 2018, UAI 2018*, 2018.

[26] Yunsheng Shi, Zhengjie Huang, Shikun Feng, Hui Zhong, Wenjing Wang, and Yu Sun. Masked label prediction: Unified message passing model for semi-supervised classification. In *International Joint Conference on Artificial Intelligence (IJCAI)*, pages 1548–1554, 2021. 2

[27] Zonghan Wu, Da Zheng, Shirui Pan, Quan Gan, Guodong Long, and George Karypis. Traversenet: Unifying space and time in message passing for traffic forecasting. *IEEE Transactions on Neural Networks and Learning Systems*, 2022. 2

[28] Jinsung Yoon, William R Zame, and Mihaela van der Schaar. Estimating missing data in temporal data streams using multi-directional recurrent neural networks. *IEEE Transactions on Biomedical Engineering*, 66(5):1477–1490, 2018. 3

[29] Joshua Ainslie, Santiago Ontañón, Chris Alberti, Philip Pham, Anirudh Ravula, and Sumit Sanghai. Etc: Encoding long and structured data in transformers. *CoRR*, abs/2004.08483, 2020. URL https://arxiv.org/abs/2004.08483. 4, 9

[30] Yu Zheng, Xiuwen Yi, Ming Li, Ruiyuan Li, Zhangqing Shan, Eric Chang, and Tianrui Li. Forecasting fine-grained air quality based on big data. In *Proceedings of the 21th ACM SIGKDD international conference on knowledge discovery and data mining*, pages 2267–2276, 2015. 4

[31] Xiuwen Yi, Yu Zheng, Junbo Zhang, and Tianrui Li. St-mvl: Filling missing values in geosensory time series data. In *Proceedings of the Twenty-Fifth International Joint Conference on Artificial Intelligence*, IJCAI'16, page 2704–2710. AAAI Press, 2016. ISBN 9781577357704. 4, 10

[32] Jacob Devlin, Ming-Wei Chang, Kenton Lee, and Kristina Toutanova. Bert: Pre-training of deep bidirectional transformers for language understanding. *arXiv preprint arXiv:1810.04805*, 2018. 4

[33] Ian R White, Patrick Royston, and Angela M Wood. Multiple imputation using chained equations: issues and guidance for practice. *Statistics in medicine*, 30(4):377–399, 2011. 8

[34] Shizhan Liu, Hang Yu, Cong Liao, Jianguo Li, Weiyao Lin, Alex X. Liu, and Schahram Dustdar. Pyraformer: Low-complexity pyramidal attention for long-range time series modeling and forecasting. In *International Conference on Learning Representations*, 2022. URL https://openreview.net/forum?id=0EXmFzUn5I. 9

[35] Diederik P Kingma and Jimmy Ba. Adam: A method for stochastic optimization. *arXiv preprint arXiv:1412.6980*, 2014. 9

[36] Guido Van Rossum and Fred L. Drake. *Python 3 Reference Manual*. CreateSpace, Scotts Valley, CA, 2009. ISBN 1441412697. 10

[37] Adam Paszke, Sam Gross, Francisco Massa, Adam Lerer, James Bradbury, Gregory Chanan, Trevor Killeen, Zeming Lin, Natalia Gimelshein, Luca Antiga, et al. Pytorch: An imperative style, high-performance deep learning library. *Advances in neural information processing systems*, 32:8026–8037, 2019. 10

[38] Matthias Fey and Jan Eric Lenssen. Fast graph representation learning with pytorch geometric. *arXiv preprint arXiv:1903.02428*, 2019. 10

[39] Andrea Cini and Ivan Marisca. Torch Spatiotemporal, 3 2022. URL https://github.com/TorchSpatiotemporal/tsl. 10

[40] neptune.ai. Neptune: Metadata store for mlops, built for research and production teams that run a lot of experiments, 2021. URL https://neptune.ai. 10

[41] David I Shuman, Sunil K Narang, Pascal Frossard, Antonio Ortega, and Pierre Vandergheynst. The emerging field of signal processing on graphs: Extending high-dimensional data analysis to networks and other irregular domains. *IEEE signal processing magazine*, 30(3):83–98, 2013. 10

Appendix

A   Performance on standard benchmarks

Table 1, in the main paper, shows the reconstruction error of the different methods as the number of valid observations in input sequences decreases. To assess the performance of our model in standard settings (denser observations), we test all the methods on the original datasets introduced in section 4. For the traffic datasets, we also consider a different evaluation mask, where data are removed according to the *Block missing* policy [6], in which we randomly mask out 5% of the available data and, in addition, we simulate failures of $S \sim \mathcal{U}(12, 48)$ consecutive steps with 0.15% probability. For this experiment, we consider also additional baselines: (1) node-level sequence mean (MEAN); (2) neighbors mean (KNN); (3) Matrix Factorization (MF); (4) MICE [33]; (5) VAR, a vector autoregressive one-step-ahead predictor; (6) rGAIN, an adversarial approach which shares similarities with GAIN [16] and SSGAN [14]. Table 2 shows the results in terms of MAE. Whenever possible, we use results from [6].

Table 2: Performance (in terms of MAE) averaged over multiple independent runs.

	Block missing		Point missing		Simulated failures	
	PEMS-BAY	METR-LA	PEMS-BAY	METR-LA	AQI-36	AQI
Mean	5.46 ± 0.00	7.48 ± 0.00	5.42 ± 0.00	7.56 ± 0.00	53.48 ± 0.00	39.60 ± 0.00
KNN	4.30 ± 0.00	7.79 ± 0.00	4.30 ± 0.00	7.88 ± 0.00	30.21 ± 0.00	34.10 ± 0.00
MF	3.28 ± 0.01	5.46 ± 0.02	3.29 ± 0.01	5.56 ± 0.03	30.54 ± 0.26	26.74 ± 0.24
MICE	2.94 ± 0.02	4.22 ± 0.05	3.09 ± 0.02	4.42 ± 0.07	30.37 ± 0.09	26.98 ± 0.10
VAR	2.09 ± 0.10	3.11 ± 0.08	1.30 ± 0.00	2.69 ± 0.00	15.64 ± 0.08	22.95 ± 0.30
rGAIN	2.18 ± 0.01	2.90 ± 0.01	1.88 ± 0.02	2.83 ± 0.01	15.37 ± 0.26	21.78 ± 0.50
BRITS	1.70 ± 0.01	2.34 ± 0.01	1.47 ± 0.00	2.34 ± 0.00	14.50 ± 0.35	20.21 ± 0.22
SAITS	1.56 ± 0.01	2.30 ± 0.01	1.40 ± 0.03	2.26 ± 0.00	18.16 ± 0.42	21.33 ± 0.15
Transformer	1.70 ± 0.02	3.54 ± 0.00	0.74 ± 0.00	2.16 ± 0.00	11.98 ± 0.53	18.11 ± 0.25
GRIN	1.14 ± 0.01	2.03 ± 0.00	$\mathbf{0.67} \pm \mathbf{0.00}$	$\mathbf{1.91} \pm \mathbf{0.00}$	12.08 ± 0.47	14.73 ± 0.15
SPIN	$\mathbf{1.06} \pm \mathbf{0.01}$	$\mathbf{1.97} \pm \mathbf{0.01}$	0.71 ± 0.01	$\mathbf{1.90} \pm \mathbf{0.01}$	$11.77 \pm \mathbf{0.74}$	$\mathbf{14.00} \pm \mathbf{0.13}$
SPIN-H	$\mathbf{1.06} \pm \mathbf{0.01}$	2.05 ± 0.03	0.74 ± 0.02	1.96 ± 0.04	$\mathbf{11.08} \pm \mathbf{0.06}$	14.39 ± 0.03

Both SPIN methods outperform the baselines in almost all scenarios. As expected, improvements are more evident when entire blocks of data are missing, as in AQI datasets and block missing settings. With respect to the spatiotemporal Transformer, SPIN performs better in all settings except for AQI-36, which can be attributed to the ineffectiveness of spatial attention alone in determining the dependencies among the different spatial locations.
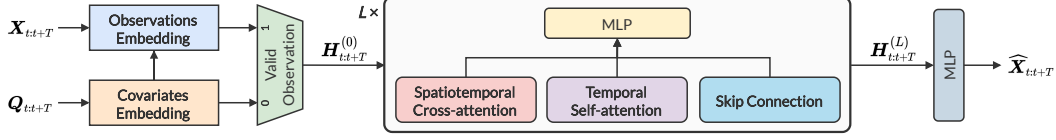
B   Hierarchical attention

In section 3 we introduced a hierarchical attention mechanism to reduce the computational complexity of the spatiotemporal attention mechanism in SPIN. In particular, such a mechanism acts by adding K hub nodes that selectively propagate information through the graph. Let $\boldsymbol{Z}^i \in \mathbb{R}^{K \times d_z}$ be the hub nodes' representations for central node i, and then, for hub k proceed as follows.

1. Update $\boldsymbol{z}_k^i$ by querying $\{\boldsymbol{h}_\tau^i \,|\, \langle \boldsymbol{x}_\tau^i, \boldsymbol{q}_\tau^i \rangle \in \mathcal{X}_{t:t+T}\}$, i.e., node encodings associated with valid observations, obtaining $\tilde{\boldsymbol{z}}_k^i$;

2. Update node encoding $\boldsymbol{h}_\tau^i$ by querying updated $\widetilde{\boldsymbol{Z}}^i$ and $\widetilde{\boldsymbol{Z}}^j$ of every j-th neighbor in $\mathcal{N}(i)$.

The spatiotemporal attention is effectively split into two phases. At first, we update each hub node representation similarly as done for the edge-level and temporal context vectors:

$$\boldsymbol{r}_{\tau,k}^i = \text{MLP}\big(\boldsymbol{h}_\tau^i, \boldsymbol{z}_k^i\big) \qquad (6)$$

$$\mathcal{R}_k^i = \{\boldsymbol{r}_{\tau,k}^i \,|\, \langle \boldsymbol{x}_\tau^i, \boldsymbol{q}_\tau^i \rangle \in \mathcal{X}_{t:t+T}\} \qquad (7)$$

$$\boldsymbol{c}_k^i = \sum_{\tau:\, \boldsymbol{r}_{\tau,k}^i \in \mathcal{R}_k^i} \alpha_{\tau,k}^i \cdot \boldsymbol{r}_{\tau,k}^i \qquad (8)$$

$$\tilde{\boldsymbol{z}}_k^i = \text{MLP}\big(\boldsymbol{z}_k^i, \boldsymbol{c}_k^i\big) \qquad (9)$$

Figure 2: The architecture of SPIN. At first, we encode observations $\boldsymbol{X}_{t:t+T}$ and spatiotemporal coordinates $\boldsymbol{Q}_{t:t+T}$, obtaining initial representations $\boldsymbol{H}^{(0)}_{t:t+T}$. The representations are updated by a stack of L sparse spatiotemporal attention blocks. Final imputations are obtained from $\boldsymbol{H}^{(L)}_{t:t+T}$ with a nonlinear readout.

Then, we obtain context vectors from the updated hub representations as:

$$\boldsymbol{r}^i_{k,\tau} = \mathrm{MLP}\big(\tilde{\boldsymbol{z}}^i_k, \boldsymbol{h}^i_\tau\big) \qquad (10) \qquad\qquad \boldsymbol{r}^{j\to i}_{k,\tau} = \mathrm{MLP}\big(\tilde{\boldsymbol{z}}^j_k, \boldsymbol{h}^i_\tau\big) \qquad (12)$$

$$\boldsymbol{c}^i_\tau = \sum_k \alpha^i_{k,\tau} \cdot \boldsymbol{r}^i_{k,\tau} \qquad (11) \qquad\qquad \boldsymbol{e}^{j\to i}_\tau = \sum_k \alpha^{j\to i}_{k,\tau} \cdot \boldsymbol{r}^{j\to i}_{k,\tau} \qquad (13)$$

and update node representation $\boldsymbol{h}^i_\tau$ as in Eq. (4). We initialize the hub representations at layer $l = 0$ with random trainable parameters. While similar methods to amortize the cost of the attention layer have been explored in different contexts [29, 34], to the best of our knowledge there are no analogous methods tackling efficient computation of spatiotemporal attention coefficients in STGNNs.

C Detailed experimental setup

In this appendix, we discuss in detail the experimental settings. We use the same setup of Cini et al. [6][3],[4]. We refer to [6] for details on these baselines.

For SPIN, we use the same hyperparameters in all datasets: $L = 4$ layers; hidden size $d_h = 32$; 2 layers with hidden size 32 for every MLP; ReLU activation functions. Masking out tokens in the target set allows SPIN to propagate only valid information. As a downside, this results in blocking the flow of information on paths through points in the target set. This can be problematic when the input observations are extremely sparse. Nonetheless, it is reasonable to assume that, after only a few propagation steps, the available information has already been partially diffused to locations with missing observations. At this point, blocked paths can be unlocked, allowing for reaching higher-order neighborhoods. In practice, we introduce a hyperparameter $\eta = 3$ to control the number of layers with masked connections and effectively split the propagation process into two phases. It is important to notice that what is being propagated in the second phase are learned representations, not observations (unavailable for masked tokens).

For SPIN-H, we use similar hyperparameters, but 5 layers (with $\eta = 3$); $K = 4$ hubs per node with $d_z = 128$ units each. These hyperparameters have been selected among a small subset of options on the validation set; we expect far better performance to be achievable with further hyperparameter tuning. Depending on the dataset, the number of parameters ranges from $\approx 55K$ to $\approx 95K$ for SPIN and $\approx 540K$ to $\approx 800K$ for SPIN-H. We use Adam optimizer [35], learning rate $lr = 0.0008$ and a cosine scheduler with a warm-up of 12 steps and (partial) restarts every 100 epochs. We train our models with 300 mini-batches of 8 random samples per epoch, fixing the maximum number of epochs to 300 and using early stopping on the validation set with patience of 40 epochs. Due to constraints on memory capacity on some of the GPUs (see the description of the hardware resources below), for SPIN-H we set the batch size to 6 and 16 in AQI and AQI-36, respectively.

To train SPIN-based models, we minimize the following loss function:

$$\mathcal{L} = \sum_{l=1}^{L} \frac{\sum_{\boldsymbol{q}^i_\tau \in \mathcal{Y}_{t:t+T}} \ell\left(\hat{\boldsymbol{x}}^{i,(l)}_\tau, \boldsymbol{x}^i_\tau\right)}{|\mathcal{Y}_{t:t+T}|}, \qquad (14)$$

where $\ell(\,\cdot\,,\,\cdot\,)$ is the absolute error and $\hat{\boldsymbol{x}}^{i,(l)}_\tau$ is l-th layer imputation for the i-th node at time step τ. Note that, to provide more supervision to the architecture, the loss is computed and backpropagated

---

[3]https://github.com/Graph-Machine-Learning-Group/grin
[4]https://github.com/TorchSpatiotemporal/tsl

w.r.t. representations learned at each layer, not only at the last one. The error is computed only on data not seen by the model at each forward pass. For this reason, we randomly remove p ratio of the input data for each minibatch sample, with p sampled uniformly from $[0.2, 0.5, 0.8]$, and use them to compute the loss. We never use data masked for evaluation to train any model.

For the spatiotemporal Transformer baseline, we use the same training strategy and a similar hyperparameters configuration of SPIN-H: $L = 5$ layers; 4 attention heads; hidden size and feed-forward size of 64 and 128 units, respectively. For SAITS, we use the code provided by the authors[5]. Hyperparameters for SAITS have been selected on the validation set with a random search by using hyperparameter ranges from the original paper.

We recall that the time and memory complexities of SPIN and SPIN-H scale with $O((N + E)T^2)$ and $O((N + E)KT)$, respectively. For the sake of comparison, here we also report the asymptotic complexities of the spatiotemporal Transformer and GRIN. The Transformer alternates temporal attention (i.e., $O(NT^2)$) and spatial attention (i.e., $O(TN^2)$), with a resulting $O((N + T)NT)$ complexity. Let R be the spatial receptive field (i.e., number of graph convolution layers) of the inner MPGRU cell, the time complexity required to process a single direction in GRIN scales with $O(TRE)$. Note also that while most of the operations in the attention-based models can be executed in parallel, GRIN would need to process the entire sequence recurrently, with a consequent performance slowdown at execution time.

All the models were developed in Python [36] using PyTorch [37], PyG [38] and Torch Spatiotemporal [39]. We use Neptune[6] [40] for experiments tracking. All the experiments have been run in a cluster using GPU-enabled nodes with different hardware setups. Running times of SPIN-H training on a node equipped with a 12GB NVIDIA Titan V GPU range from 4 to 14 hours (depending on the dataset). For SPIN we used a node with 40GB NVIDIA A100 GPU, with running times ranging from 4 to 26 hours.

D Datasets

In this appendix, we provide details on datasets and preprocessing used for the experiments. We use temporal windows of $T = 24$ steps for all datasets except AQI-36, for which we set $T = 36$. For traffic datasets, we split the data sequentially as 70% for training, 10% for validation, and 20% for testing. For air quality datasets, following Yi et al. [31], we consider as the test set the months of March, June, September, and December and we use valid observation x_τ^i as ground-truth if the value is missing at the same hour and day in the following month. For data preprocessing we use the same approach of Cini et al. [6], by normalizing data across the feature dimension (graph-wise for graph-based models) to zero mean and unit variance.

In line with [3, 6], we obtain the adjacency matrix from the node pairwise geographical distances using a thresholded Gaussian kernel [41]

$$a^{i,j} = \begin{cases} \exp\left(-\frac{\text{dist}(i,j)^2}{\gamma}\right) & \text{dist}(i,j) \leq \delta \\ 0 & \text{otherwise} \end{cases}, \tag{15}$$

where $\text{dist}(\cdot, \cdot)$ is the geographical distance operator, γ is a shape parameter and δ is the threshold.

Note that we considered settings where the topology is static. The extension to dynamic graphs, where $\boldsymbol{A} = \boldsymbol{A}_t$ and $N = N_t$, can be an interesting future work while being outside the scope of this paper.

E Ablation study

Table 3 shows the results of an ablation study on METR-LA (Point missing) and AQI-36. Here, we evaluate the performance in terms of mean absolute error (MAE) and mean relative error (MRE). We consider two different versions of SPIN-H in which we remove the spatiotemporal cross-attention and the temporal self-attention components, respectively. We also report the performance of SPIN, SPIN-H and the Transformer for reference. Results clearly show that both components contribute

---

[5]https://github.com/WenjieDu/SAITS
[6]https://neptune.ai/

Table 3: Ablation study to assess the contribution of the single components in the spatiotemporal attention block. Performance averaged over multiple independent runs.

	METR-LA (P)		AQI-36	
	MAE	MRE (%)	MAE	MRE (%)
SPIN	**1.90** $_{\pm\,0.01}$	**3.29** $_{\pm\,0.01}$	**11.77** $_{\pm\,0.74}$	**16.56** $_{\pm\,1.05}$
SPIN-H	1.96 $_{\pm\,0.04}$	3.39 $_{\pm\,0.06}$	**11.08** $_{\pm\,0.06}$	**15.60** $_{\pm\,0.09}$
Without cross-attention	2.18 $_{\pm\,0.01}$	3.78 $_{\pm\,0.01}$	15.36 $_{\pm\,0.09}$	21.62 $_{\pm\,0.13}$
Without self-attention	2.24 $_{\pm\,0.09}$	3.88 $_{\pm\,0.16}$	13.63 $_{\pm\,0.23}$	19.19 $_{\pm\,0.32}$
Transformer	2.16 $_{\pm\,0.00}$	3.74 $_{\pm\,0.01}$	11.98 $_{\pm\,0.53}$	16.87 $_{\pm\,0.75}$

positively to imputation accuracy. We also point out that in METR-LA (P) observations are masked out uniformly at random while the mask in AQI-36 reflects the empirical distribution of missing data in the dataset.